BIOCHEMISTRY
including biophysical chemistry & molecular biology

Article

pubs.acs.org/biochemistry

A Pearl Protein Self-Assembles To Form Protein Complexes That Amplify Mineralization

Iva Perovic,[†] Trinanjana Mandal,[‡] and John Spencer Evans*[,†]

[†]Laboratory for Chemical Physics, Division of Basic Sciences and Craniofacial Biology, New York University, 345 E. 24th Street, NY, New York 10010, United States

[‡]Department of Chemistry and the Molecular Design Institute, New York University, 100 Washington Square East, New York, New York 10003-6688, United States

Supporting Information

ABSTRACT: The formation of the nacre pearl in marine invertebrates represents an on-demand production of mineralization in response to an irritant or parasite threat to the mantle organ. In the Japanese pearl oyster (*Pinctada fucata*), this process is mediated by a 12-member protein family known as PFMG (*Pinctada fucata* mantle gene). One of these proteins, PFGM1, has been implicated in modulating calcium carbonate crystal growth and has been reported to possess an EF-hand-like domain. In this report, we establish that the recombinant PFMG1 (rPFMG1) is an intrinsically disordered "imitator" EF-hand protein that increases the number of calcium carbonate mineral crystals that form relative to control scenarios and does not induce aragonite formation. This protein possesses a modified pseudo-EF-hand sequence at the C-terminal end which exhibits low homology (30−40%) to the pseudo-EF-hand mitochondrial SCaMCs buffering/solute transport proteins. This low sequence homology is the result of the inclusion of disorder-promoting amino acids and short amyloid-like aggregation-prone cross-β-strand sequences within the putative PFMG1 pseudo-EF-hand sequence region. Similar to other nacre proteins, rPFMG1 oligomerizes to form amorphous, heterogeneously sized protein oligomers and films *in vitro*, and this process is enhanced by Ca^{2+}, which promotes the formation of aggregation-prone extended β-strand structure within rPFMG1. From these results, we conclude that PFMG1 forms supramolecular assemblies that play an important role in amplifying the nucleation process that is crucial for coating or neutralizing invasive threats to the mantle organ.

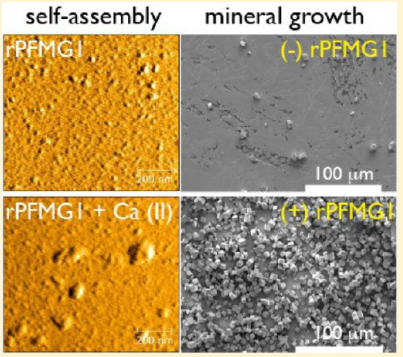

The formation of biominerals in nature often requires the participation of specialized proteins that direct matrix assembly, nucleation, and crystal growth.[1−12] In many cases, the sequences of these specialized proteins are highly unique and often feature regions that do not correspond to the sequences of other known globular proteins.[1−11] However, there exist imperfect sequence homologies (i.e., < 50%) between certain regions of intrinsically disordered[13−15] biomineralization proteins and other nonmineral associated proteins.[1,3−5] We will refer to these imperfect homologous domains as "imitator" domains, since they copy certain aspects of the globular sequence with less than perfect fidelity. Some recent examples have been identified in mollusk shell mineralization protein sequences, where regions partially homologous to RING-like sequences,[5] acetylcholine-binding domains,[3] glycine loops,[1] and disulfide core domains[1] exist. Because of a number of factors, little if any information is available regarding the true function of these imitator domains within biomineralization proteins. However, there is speculation that these domains act as nucleation and crystal growth regulators or participate in other matrix functions.[3,5]

One interesting example of an imitator domain-containing biomineralization protein is PFMG1 (*Pinctada fucata* mantle gene) (116 AA, MW = 13 609 Da, pI = 7.93) (Figure 1A).[3] This protein is a member of the 12 PFMG proteins secreted by the outer epithelial cell layer of mantle tissue in the Japanese pearl oyster, *Pinctada fucata*.[3] These proteins are implicated in the formation of the pearl nacre, and recent studies with PFMG1 indicate that this particular protein influences the nucleation of calcium carbonates *in vitro* compared to negative control assays.[3] It has been reported that the C-terminal region of PFMG1 exhibits partial homology (<40%) to EF-hand Ca^{2+} binding domains (Figure 1B).[16−22] However, note that there are two EF-hand protein families that are functionally and structurally distinct. The canonical EF-hand proteins (e.g., calmodulin and calbindin) are involved in signaling and typically undergo a calcium-dependent conformational change which opens a target binding site.[16−18,20] Conversely, the pseudo-EF-hand proteins (e.g., S100) are responsible for buffering or ion transport and do not undergo calcium-dependent conformational changes.[19,21,22] Hence, the PFMG1 protein could be an "imitator" protein that mimics one of these two EF-hand families as part of its participation in the pearl formation process. However, very little is known regarding

Received: June 22, 2013
Revised: July 17, 2013
Published: July 18, 2013

   dx.doi.org/10.1021/bi400808j | *Biochemistry* 2013, 52, 5696−5703

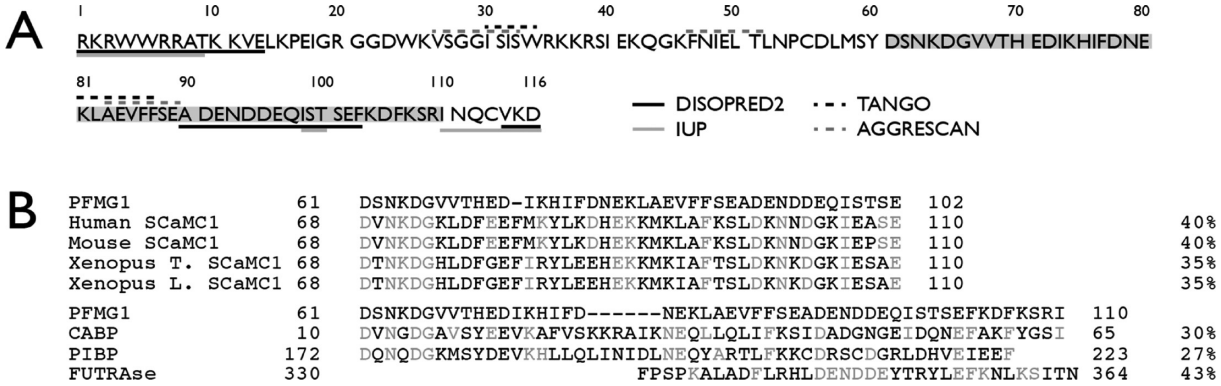

Figure 1. (A) Bioinformatics analysis of the PFMG1 primary sequence (UniProt accession number Q3YL59). Disordered sequence regions (solid lines) were identified using IUP_PRED and DISOPRED2 prediction algorithms, and cross-β-strand sequence regions (dashed lines) which exhibit association propensities were identified using TANGO and AGGRESCAN. The gray highlighted region represents the putative EF-hand domain. (B) BLAST sequence alignment of PFMG1 with other EF-hand protein sequences. Gray residues denote homologies with PFMG1. The SCaMC1 proteins are members of the pseudo-EF-hand family.

PFMG1 function and structure, and hence it is not clear how this biomineralization protein, or its putative EF-hand region, should be classified.

In this paper we report new experiments which establish the functional and structural relevance of PFMG1 and its putative EF-hand region with regard to the pearl biomineralization process. Specifically, we document the ability of recombinant PFMG1 (rPFMG1) to boost the nucleation process as exhibited by increased *in vitro* crystal production with no evidence of polymorph (aragonite) formation. We also discovered that rPFMG1, like other nacre-associated proteins, is intrinsically disordered, exhibits unique pH- and Ca^{2+}-dependent aggregation-prone behavior in solution, and self-assembles to form heterogeneously sized protein oligomers under mineralization conditions. Using bioinformatics, we confirm a 30−40% sequence homology between the C-terminal region of PFMG1 (positions 61−110) and the pseudo-EF-hand domains of small calcium-binding mitochondrial carrier (SCaMCs) subfamilies that possess solution buffering capabilities.[19,21,22] Hence, PFMG1 is an aggregation-prone pseudo-EF-hand "imitator" protein that amplifies the nucleation process during pearl formation.

EXPERIMENTAL PROCEDURES

Synthesis and Purification of rPFMG1. The gene synthesis, cloning, bacterial expression, and purification of rPFMG1 were performed by GenScript USA (Piscataway, NJ) using their proprietary OptimumGene system and recombinant expression systems. The synthetic DNA was created from the complete PFMG1 sequence (UniProt accession number Q3YL59) minus the membrane leader sequence (residues 1−20) yielding a target sequence of 116 AA that now starts at residue 21 (new N-terminus, R1) and ends at residue 136 (now D116) (Figure 1A). To this DNA sequence a hybrid poly(His)$_6$ tag−enterokinase (EK) protease cleavage site was incorporated at the N-terminus to facilitate the purification of rPFMG1 in a one-step fashion using high-affinity Ni chelation chromatography followed by enzyme digestion/affinity removal. The recombinant plasmid was transiently transfected into a 100 mL suspension of HEK 293 cell culture, which was then grown in serum-free media, collected, and lysed at day 5 post-transfection. Cell pellets were resuspended in phosphate buffered saline (PBS) and sonicated for 2 min to reduce solution viscosity. The solution was then centrifuged, and the target protein was captured from the cell lysate using HiTrap chelating Ni HP column and eluted with 200 mM imidazole buffer.

Following Ni elution, poly(His)$_6$ tag removal was accomplished via EK digestion and subsequent affinity capture of the EK enzyme. The final protein purity was determined to be 93% (4%−20% gradient SDS-PAGE/Coomassie Blue staining, reducing conditions). The minor impurity was determined to be an aggregate of the rPFMG1 protein (>100 kDa), which was subsequently removed from the protein sample via ultrafiltration (Amicon Ultra 0.5, 30 kDa MWCO, Millipore Corporation) at 14 000 rpm, 15 min, and 25 °C, with rPFMG1 recovered in the flow-through supernatant. Using a Bruker Daltonics MALDI-TOF, we determined the apparent MW of this purified material to be 13 625 kDa (Figure S1, Supporting Information), which is close to the hypothetical MW of 13 609 Da. Purified protein stock aliquots were stored in 50 mM Tris-HCl/10% v/v glycerol (pH 8.0) at −80 °C until needed. For subsequent experimentation, rPFMG1 samples were created by exchanging and concentrating appropriate volumes of stock solution into unbuffered deionized distilled water (UDDW) or other appropriate buffers using Amicon Ultra 0.5, 3 kDa MWCO (Millipore Corporation).

Calcium Carbonate Nucleation. Using the same assay conditions employed in nacre protein−aragonite formation studies (16 h, 16 °C, 12.5 mM $CaCl_2$, with the final pH = 8.0−8.3 at the conclusion of the assay), we monitored the effect of rPFMG1 on calcium carbonate crystal growth using standard solid ammonium carbonate vapor decomposition methods.[8,11,12,23,24] These assay solutions contained either no protein (negative control) or final assay concentrations of 0.7, 1.8, 3.7, and 7.3 μM rPFMG1 protein. The collection procedure for SEM analysis of assay precipitates involved the use of Si wafer fragments (1 cm^2 or less in size, "P" type [1 0 0], 20 ohm·cm, 250−350 μm, Silicon Quest Intl., Santa Clara, CA) or freshly cleaved geologic calcite fragments (Iceland spar, no larger than 3 mm × 3 mm) that were placed at the bottom of the wells prior to the start of the assay.[5,8] Si wafers and calcite fragments containing assay deposits were washed with calcium carbonate saturated methanol and then dried at 37 °C overnight. For SEM imaging dried Si wafer or calcite fragment samples were coated with a thin layer of gold and then imaged using a Hitachi S-3500N scanning electron microscope (5 kV)

dx.doi.org/10.1021/bi400808j | *Biochemistry* 2013, 52, 5696−5703

utilizing secondary emission detection. Energy dispersive spectra (EDS) were collected on carbon-coated samples using the PGT-Bruker X-ray microanalysis system at 25 kV.

Dynamic Light Scattering. The hydrodynamic radii of rPFMG1 complexes were measured over a pH range of 7−10.5 using a DynaPro MS/X dynamic light scattering instrument (Protein Solutions, Inc.) and experimental protocols developed for nacre polypeptides.[11,24,25] Using 10 mM buffers (pH 7.0−8.5, Tris-HCl buffer; pH 9.0−10.5, sodium carbonate−bicarbonate buffer), we created final rPFMG1 concentrations = 3.7, 7.3, 20, 50, 75, and 100 μM, which correspond to the concentration range utilized in earlier nacre protein self-association DLS studies.[11,24,25] All samples were filtered using 0.22 μm poly(vinylidene fluoride) syringe filter (Fisher Scientific) and then incubated at 16 °C (same temperature as for mineral assays) for 5 min in the cuvette prior to measurement.[11,22,24,25] Studies conducted below pH 7 led to excessive spontaneous protein precipitation, and for this reason were excluded from our analysis. Ten acquisitions were taken per pH point per sample. Data regularization analysis was performed using the Dynamics v6.0 software. By measuring the fluctuations in the laser light intensity scattered by the sample, the instrument is able to detect the speed (diffusion coefficient) at which the particles are moving through the medium.[26]

X-ray Diffraction. Washed and dried control and rPFMG1 precipitates from mineralization assays were analyzed using a Bruker D8 DISCOVER GADDS microdiffractometer equipped with a VANTEC-2000 area detector in a φ rotation method. The X-ray generated from a sealed copper tube is monochromated by a graphite crystal and collimated by a 0.5 mm MONOCAP (λ Cu Kα = 1.541 78 Å). The sample−detector distance is 150 mm. Two runs with $\theta_1 = \theta_2 = 15°$ and 30° are collected for each specimen, and the exposure time is 600 s per run. Data were merged and integrated by the XRD2EVAL program in the Bruker PILOT software. The composition of calcium carbonate polymorphs was calculated in each sample with reference to calcite, aragonite, and vaterite-specific X-ray diffraction data that were obtained from the Power Diffraction File (PDF), a database of X-ray powder diffraction patterns maintained by the International Center for Diffraction Data (ICDD).

AFM Imaging of rPFMG1 Assemblies. To complement our DLS studies, we investigated the dimensional and morphological characteristics of rPFMG1 assemblies captured from solution onto mica substrates. AFM experiments were executed at 25 °C using an Asylum MFP-3D standalone AFM operating in tapping mode in buffer solution. V-shaped Si_3N_4 cantilevers (reported spring constant 0.09 N/m) were used for imaging. A precise drive frequency in fluid (8 kHz) was calculated for each cantilever prior to imaging by overlaying the thermal spectrum over the frequency sweep. Two rPFMG1 samples were imaged: an apo sample (7.3 μM in 10 mM Tris-HCl, pH 8.0) and a Ca(II)-loaded sample (7.3 μM in 10 mM Tris-HCl, 12.5 mM $CaCl_2$, pH 8.0). All samples were delivered onto a freshly stripped surface of mica (Ted Pella, Inc., 0.9 mm thick) and incubated for a period of 15 min at ambient temperature prior to measurement. Igor Pro 6.01 software was used for image acquisition at a scan rate of 2 Hz. Gwyddion software[27] was implemented for image processing, noise filtering, and analysis.

Circular Dichroism Spectrometry. CD spectra (190−260 nm) of r-PFMG1 in 10 mM Tris pH 8.0 and in the presence of $CaCl_2$ were collected at 25 °C on the AVIV stopped flow 202SF CD spectropolarimeter. A total of eight scans per sample were collected in a cuvette with 0.1 cm path length, using 1 nm bandwidth, 1 nm wavelength step, and 0.5 s averaging time. The instrument was previously calibrated with D-10-camphor-sulfonic acid. Initial CD studies examined a range of concentrations from 0.7 to 7.3 μM. Calcium titrations were performed in 10 mM Tris pH 8.0, using 7.3 μM protein samples that contained Ca^{2+}:protein mole ratios of 1:2, 1:1, 2:1, 10:1, and 1700:1 (i.e., 12.5 mM $CaCl_2$). The recorded spectra were averaged and the appropriate background spectra (Tris buffer with and without $CaCl_2$) subtracted. Spectra were smoothened using the binomial algorithm included in the AVIV CD software. Ellipticity is reported as mean residue ellipticity (deg cm^2 dmol^{-1}). Secondary structure estimates of rPFMG1 samples were obtained using three different algorithms included in the CDPro software package (SELCON3, CDSSTR, CONTILL) and the SMP56 Reference Protein Set.[28−30]

Bioinformatics. The Basic Local Alignment Search Tool (BLAST, National Center for Biotechnology Information) and InterProScan/SWISS MODEL programs (SwissProt) were used to determine the sequence homology between PFMG1 and protein database EF-hand protein sequences (Figure 1B).[31−33] To determine the location of disordered sequence regions within the PFMG1 sequence, we employed the IUP_PRED[34] and DISOPRED2[35] prediction algorithms using default parameters. Subsequently, we utilized TANGO[36] and AGGRESCAN[37] to globally identify putative cross-β-strand sequence regions which exhibit association propensities.

RESULTS

Crystal Growth Experiments Reveal That rPFMG1 Is a Nucleation Enhancer. In previous light microscopy studies, a recombinant version of PFMG1 was demonstrated to affect calcium carbonate crystal growth.[3] However, smaller length scale measurements and quantitative analysis were not performed on these deposits, and so the *in vitro* function of this protein was not firmly established. Using standard ammonium carbonate vapor diffusion mineralization assays, we extend this knowledge and find that rPFMG1 enhances the nucleation of calcite crystals *in vitro* (Figure 2 and Figure S2). Compared to control assays (no protein added), we observe that the number of rhombohedral single and polycrystalline calcite crystals increases as a function of rPFMG1 concentration. At the same time, we note that calcite crystal dimensions diminish (Figure 2). These rPFMG1-generated mineral deposits were confirmed to be calcite (powder X-ray diffraction, Figure 3), with no detectable evidence of vaterite or aragonite formation. Thus, rPFMG1 increases the number of nucleating mineral clusters at the expense of mineral cluster size, with no evidence of polymorph selection; i.e., the protein acts as a nucleation enhancer.

A high-magnification comparison of the mineral crystal surfaces obtained in both the negative control and rPFMG1 assays (Figure S3) reveals that control and rPFMG1 assay mineral samples have similar surface morphologies. Thus, under these assay conditions,[2,4,5,11,12] rPFMG1 does not appear to alter calcite crystal morphologies or surfaces to a significant degree. These findings correlate with our X-ray microanalyses, where we were unable to detect rPFMG1 protein on the surface of these crystals (via Cys-specific thiol S detection, Figure S4). Understandably, the fact that our mineral surfaces are rough in texture and that PFMG1 contains only two Cys residues (Figure 1A) prevents us from conducting an accurate

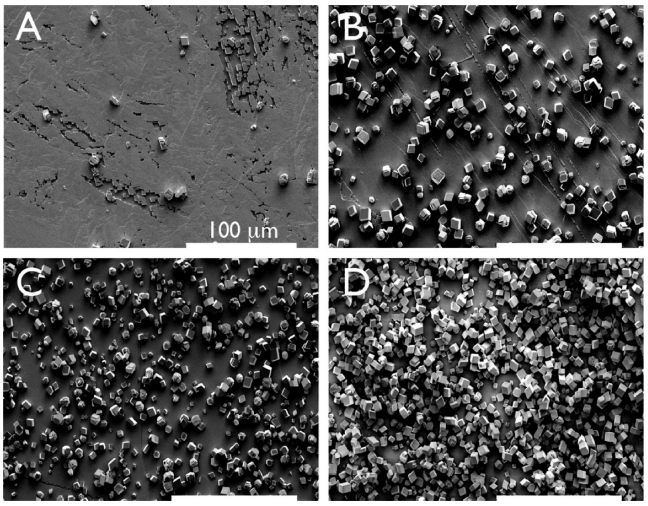

Figure 2. Scanning electron micrograph of mineral deposits captured by geologic calcite fragments in ammonium carbonate vapor diffusion mineralization assays. (A) Protein-free assay (negative control). Note predominance of single crystal and polycrystalline calcite crystals. (B, C, D) 1.8, 3.7, and 7.3 μM rPFMG1 assays, respectively. Note that as rPFMG1 concentrations increase, the number of calcite crystal increases. Scale bars = 100 μm.

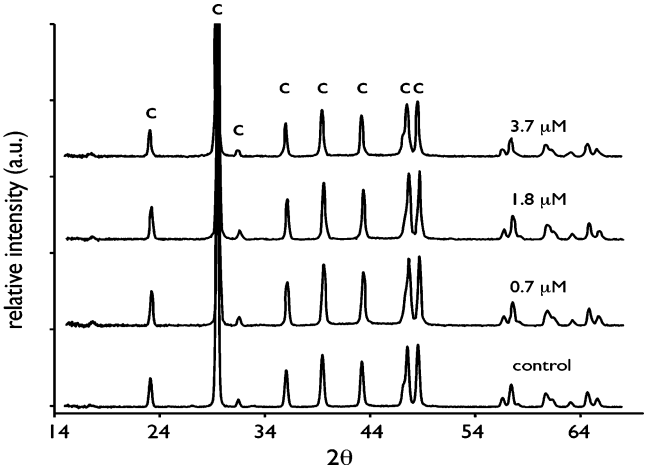

Figure 3. Representative powder micro-X-ray diffraction spectra of Si wafers taken from protein-free (control) and rPFMG1-containing mineralization assays. Calcite (c) reference peaks are denoted and were obtained from known data sets (International Center for Diffraction Data (ICDD)). Note that diffraction data for 7.3 μM rPFMG1 is identical to that obtained for 3.7 μM.

quantitative analysis. Thus, our SEM and X-ray microanalysis date point to several possibilities: (a) the adsorption of rPFMG1 onto calcite crystal surfaces is either very low or nonexistent (Figures S3 and S4); (b) the protein may be adsorbed onto crystal surfaces, but due to the low S content in the protein, it is not possible to detect adsorbed rPFMG1; (c) the protein may be entrapped within the crystals and thus unavailable for surface detection by X-ray microanalysis.

rPFMG1 Oligomerizes in Solution To Form Heterodisperse Supramolecular Assemblies. It is known that some nacre-associated proteins spontaneously form mineral-stabilizing protein oligomers in solution.[11,12,23−25,38,39] Using dynamic light scattering (DLS), we find that the same holds true for the pearl protein, rPFMG1 (Figure 4). At rPFMG1 concentrations corresponding to those utilized in our assays (7.3 μM, Figure 2), we observe that rPFMG1 oligomerizes over the pH range 7−10.5 (Figure 4 and Figure S5). At all pH points there is significant size heterogeneity as evidenced by polydispersity values >15% (represented by error bars on each histogram bar). On the basis of mass percent, two oligomer populations are noted at pH = 7, 9, 10, and 10.5 with hydrodynamic radii (R_H) values ranging from 4.7−7.6 nm and 27.7−48.2 nm. At pH 8.0, which coincides with the mineralization assay pH and the pI of PFMG1, a single oligomer population is noted (R_H = 75 nm), and this represents the largest apo-rPFMG1 oligomer that we can detect with DLS. In contrast, three populations exist at pH 9.5 (R_H = 2.6, 7.4, and 47.3 nm; Figure 4). The variations in mass percent and particle size suggest that rPFMG1 oligomerization is pH-dependent, and thus protein electrostatics plays a role in the self-assembly process.

We next explored rPFMG1 self-assembly in the presence of Ca^{2+} at pH 8.0 (Figures S6 and S7). At all stoichiometries there is significant size heterogeneity as evidenced by polydispersity values >15%. At Ca^{2+}:protein stoichiometries of 1:1 and 2:1, we observe three rPFMG1 oligomer populations, and at all other stoichiometry points we observe two oligomer populations. In general, Ca(II)-induced oligomer dimensions (R_H = 4−20 nm, 40−64 nm) exceed those obtained for the apo state (Figure 4). Hence, rPFMG1 self-assembles to form heterodisperse oligomers over a wide pH range, with a higher degree of oligomerization noted in the presence and absence of Ca^{2+} at pH 8.0 (Figure 2).

rPFMG1 Oligomerization Is Enhanced by Ca^2 and Promotes Protein Film Formation. Our DLS experiments can only detect submicrometer-sized protein assemblies, and potentially any oligomers >0.2 μm would be purged via filtration. To probe beyond this limit, we performed tapping mode AFM imaging of 7.3 μM rPFMG1 protein oligomers that settle onto untreated mica substrates (Figure 5) under conditions reflecting assay scenarios (Figure 2) and highest particle sizes (Figure 4). In the apo state, we confirm the formation of heterogeneously sized amorphous-appearing oligomers that are spherical to ellipsoidal in morphology (Figure 5). Using line profile extraction of amplitude and height images of 10 typical oligomers, we estimate that apo-rPFMG1 protein oligomers possess average diameters = 31 ± 9 nm and heights = 1 ± 0.7 nm. With the introduction of Ca^{2+}, we now observe larger complexes and evidence of particle fusion with average diameters = 86 ± 34 nm (2−2.25-fold increase) and heights = 6 ± 3 nm (3−4-fold increase) for individual complexes (Figure 5). Thus, we confirm our DLS findings, namely, that rPFMG1 possesses self-associative capabilities that are enhanced by Ca^{2+}.

The apo-rPFMG1 oligomers appear contiguous and suggest that a film-like protein coating is forming on the mica surface, with larger particles projecting above the film layer (Figure 5). To confirm this, we measured the R_q, or root-mean-square surface roughness, of a freshly cleaved mica surface in buffer (R_q = 0.078 nm) versus untreated mica surfaces exposed to apo-rPFMG1 (R_q = 0.17 nm, ∼2-fold increase) and rPFMG1 in 12.5 mM $CaCl_2$ (R_q = 0.26, ∼3-fold increase) and confirmed that under apo and Ca^{2+} conditions the mica surfaces are coated with rPFMG1 oligomers. Other calculated surface parameters [i.e., roughness average (R_a), maximum roughness (R_p)] were found to exhibit similar trends between plain mica and rPFMG1-treated mica (data not shown), and this confirms

dx.doi.org/10.1021/bi400808j | Biochemistry 2013, 52, 5696−5703

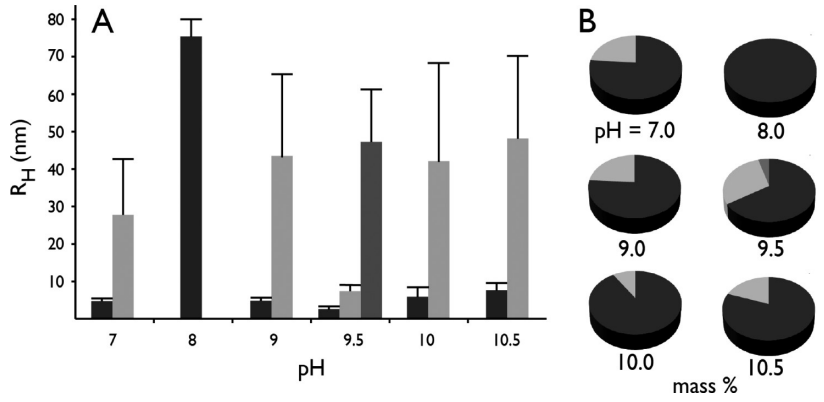

Figure 4. Dynamic light scattering analysis of r-PFMG1 oligomerization (7.3 μM) in various pH buffers at 16 °C. (A) Hydrodynamic radii determined for distinct oligomer populations as defined in Figure S5. Error bars represent polydispersity of particle sizes obtained for each pH. (B) Pie chart representation of distinct oligomer populations and corresponding mass % as a function of pH. Mass % and corresponding R_H radii are matched by comparable grayscale shading of pie charts and histogram bars.

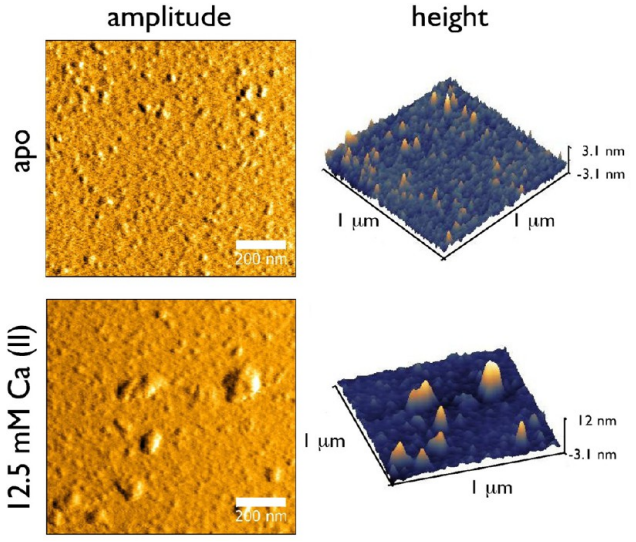

Figure 5. Tapping mode AFM images of 7.3 μM rPFMG1 protein oligomers (10 mM Tris-HCl, pH 8.0) in the presence and absence of 12.5 mM $CaCl_2$ on untreated mica surfaces. Note in the height plots that the rPFMG1 oligomers form a contiguous film-like layer or coating on the mica surface.

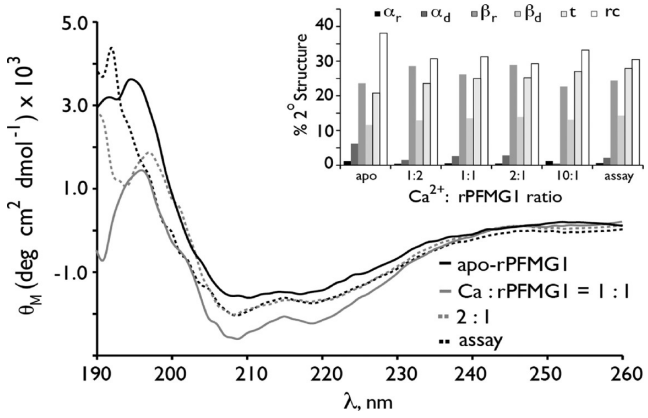

Figure 6. Circular dichroism spectra of 7.3 μM oligomeric rPFMG1 (10 mM Tris-HCl buffer, pH 8.0) in the presence and absence of stoichiometric levels of $CaCl_2$. "Assay" refers to 12.5 mM $CaCl_2$ (i.e., Ca^{2+}:rPFMG1 1700:1). Inset histogram plot details % secondary structure content determined by CDPro (CDSSTR) and the SMP56 Reference Protein Set.[28−30] The histogram data are reported as fractional weight distributed between regular helix (α_r), distorted helix (α_d), regular strand (β_r), distorted strand (β_d), turn (t), and random coil or unordered (rc) structures.

the formation of a protein coating or film comprised of oligomers on these mica surfaces.

Structural Features of Oligomeric rPFMG1. Earlier studies with oligomeric nacre-associated proteins demonstrated the presence of intrinsic disorder that persists in the assembled state.[4,9,11,12,23−25,38,39] Since rPFMG1 spontaneously forms protein assemblies (Figures 4 and 5), it is likely that disordered regions are present in this protein, but this has yet to be established. Moreover, canonical and pseudo-EF-hand proteins possess specific structural features in the presence and absence of Ca^{2+},[16−20] and to date no specific studies have established which structural features are found in PFMG1.

To remedy this, we first performed circular dichroism (CD) spectrometry on apo-rPFMG1 protein oligomer samples (i.e., 7.3 μM rPFMG1, 10 mM Tris-HCl, pH 8.0). Here, we find that the CD spectra for rPFMG1 oligomers feature a (+) ellipticity band with a maxima at 187 nm and three broad (−) ellipticity bands with minima at 208, 215, and 220 nm (Figure 6). With 208 nm/222 and 215 nm being characteristic for α-helix and β-strand, respectively,[8,9,11,12,28−30] it is clear that rPFMG1 assemblies are comprised of protein molecules that possess residual structure.[8,9,11,12] However, since these bands are broad and weak in intensity, it is likely that the protein contains some degree of unfolding or disorder.[8,9,11,12,28−30] This is confirmed by comparison to CD database reference spectra (CDSSTR, SMP56, inset, Figure 6) where rPFMG1 can be characterized as approximately 38% random coil, 21% turn, 35% total β-strand, and 6% helix.[28−30] We stress caution when interpreting these results as absolute values and prefer to rely on them in relative terms. Nonetheless, we note that the low content of α-helical structure is atypical for folded EF-hand proteins that contain a stable 4-helix bundle.[16−20] Hence, on a structural basis, we conclude that rPFMG1 is intrinsically disordered and does not fit the description of a true canonical 4-helix bundle EF-hand protein.

Next, to qualitatively classify the type of putative EF-hand domain sequence in PFMG1, we utilized stoichiometric Ca^{2+} titration in tandem with CD to determine the Ca^{2+}-induced conformational response of rPFGM1 within assemblies (Figure

6). Compared to the apo-state, we note that CD band intensities initially increase at Ca^{2+}:protein = 1:1 but then diminish as Ca^{2+} levels increase. We attribute this reduction in molar ellipticity intensities to increases in either protein assembly dimensions or populations (Figure 5; Figures S6 and S7) that would lead to increased beam scattering and subsequent loss in signal intensities. In terms of secondary structure content, we note that at Ca^{2+}:protein = 1:1 the random coil and helix contents decrease relative to the apo-state. Simultaneously we note concomitant increases in β-strand and turn structures relative to the apo-state. At Ca^{2+}:protein ratios >1:1 we note that these trends persist and that there are no further changes in secondary structure content (Figure 6), even when we reach mineral assay levels (12.5 mM or 1700:1). We conclude the following: (a) The structural response of rPFMG1 to Ca^{2+} is similar to that described for pseudo-EF-hand proteins, i.e., limited conformational sensitivity to Ca^{2+};[18−21] (b) Ca^{2+} induces increases in β-structures within rPFMG1 at the expense of helical and random coil contents, and since β-structures are associated with aggregation,[36−38] this explains why rPFMG1 forms larger aggregates and films in the presence of Ca^{2+} compared to the apo-state (Figure 5; Figures S6 and S7).

Bioinformatics Confirm That PFMG1 Is a Pseudo-EF-Hand Protein That Possesses Intrinsically Disordered and Aggregation-Prone Regions. It is known that nacre extracellular matrix proteins possess two types of sequence characteristics that promote self-association: intrinsic disorder/unfolding and amyloid-like aggregation prone cross-β-strand supersecondary structures.[38] Using predictive algorithms IUP and DISOPRED, we identified an intrinsically disordered region in both the N-terminal and C-terminal domains of PFMG1 (Figure 1A). Interestingly, the predicted region of disorder in the C-terminal domain overlaps with a 13 AA sequence region that comprises the putative EF-hand domain (3). The presence of disorder in this region may explain why rPFMG1 possesses a lower α-helical content compared to other EF-hand proteins (Figure 6).[16−22] Similarly, using predictive algorithms TANGO and AGGRESCAN for identifying aggregation-prone cross-β-strand sequences, we identified three putative regions (representing 22% of the total sequence length) at positions 26−34, 46−52, and 81−89 (coinciding with the EF-hand region) (Figure 1A). Once again, there exists overlap between a predicted assembly domain and the EF-hand domain.[3] The prediction of 22% extended β-strand content roughly correlates with the detection of regular (20%) and distorted (14%) β-strand content detected by CD spectrometry (Figure 6). Thus, the PFMG1 protein contains intrinsically disordered and aggregation-prone sequences, with examples of each sequence type found within the putative EF-hand domain.

The occurrence of aggregation-prone sequence features within the PFMG1 EF-hand region provides the context for a re-examination of sequence homology of this protein (Figure 1B). Initial homology studies reported that PFMG1 exhibited 40% homology with the EF-hand calcium binding protein, CBP-1,[3] but no other homologous sequences were reported at that time. Using BLAST and InterProScan/SWISS MODEL, we identified seven additional pseudo-EF-hand protein sequences that are homologous (27−43%) to PFMG1 (Figure 1B). This list of proteins includes fucosytransferases (FUTRAse), phosphodiesterases (PIBP), calcium binding protein (CaBP), and solute carrier calcium-binding mitochondrial carriers (SCaMCs) subfamilies that act as buffering agents.[19,21,22] Note that the SCaMCs exhibit the best homology match to the putative PFMG1 EF-hand sequence region, and thus PFMG1 appears to be a pseudo-EF-hand "imitator" protein whose sequence region are more closely related to the solution buffering protein families.[19,21,22]

Interestingly, we note that the PFMG1 regions that exhibit the lowest homology to SCaMCs possess aggregation-prone and intrinsically disordered features. Specifically, the -KLAE-VFFSEA- region (residues 81−90, 27% homology) is predicted to be an amyloid-like aggregation-prone sequence (Figure 1B). Conversely, the -ADENDDEQISTSE− region (residues 90−102, 46% homology) is predicted to be an intrinsically disordered sequence (Figure 1) due to the introduction of disorder-promoting residues[13−15,39] E, D at sequence positions 92, 94, 96, and S, Q at positions 99 and 97, respectively (Figure 1B). We believe that the disordered and aggregation prone regions within the PFMG1 pseudo-EF-hand sequence have altered the functional properties of this SCaMCs-related domain, such that this sequence region can participate in protein−protein interactions (Figure 5) and protein−mineral modulation (Figure 2).

■ DISCUSSION

The formation of a natural pearl initiates when a foreign substance or parasite becomes trapped between the shell nacre layer and the mantle organ of the mollusk.[40] This triggers cellular migration and encapsulation around the irritant, followed by the release of the "maintenance crew" (i.e., mantle proteins that initiate a new cycle of nacre formation) into the encapsulated space around the irritant. Ultimately, a new layer of nacre (pearl) is created around the irritant, rendering it harmless to the mantle organ. The PFMG protein family is a part of this "crew", and as we have demonstrated in this report, PFMG1 protein potentially plays an important part in the nacre deposition process. Our *in vitro* mineralization experiments confirm that oligomeric PFMG1 is a nucleation enhancer (Figure 2 and Figure S2) that increases the number of calcium carbonate crystals formed relative to control scenarios yet does not participate in aragonite selection/stabilization (Figure 3; Figures S3 and S4). Within the context of pearl formation[40] and the current prenucleation cluster hypothesis,[41−43] we believe that oligomeric PFMG1 rapidly induces mineral formation in order to ensure that the irritant becomes rapidly coated and neutralized. Hypothetically, this could be accomplished by increasing the number of prenucleation clusters that are formed in solution.[42,43] This would give rise to a larger number of smaller-sized ACC clusters, which, in turn, would result in the generation of more crystals with smaller dimensions compared to control scenarios (Figure 2). Clearly, additional experimentation will be required to delineate the pearl nacre formation process in more detail.

In earlier studies we investigated the mineralization activities of the N- and C-terminal 30 AA regions of PFMG1 using model peptides.[45] We found that both sequences form peptide assemblies under mineralization assay conditions similar to those employed in the present study. Furthermore, both peptide sequences possessed secondary structure characteristics that are also similar to those found in rPFMG1 (Figure 6). However, the notable difference between rPFMG1 and these two model peptides lies in their mineralization activities: While rPFMG1 amplifies crystal deposition and does not affect crystal morphologies, both of the PFMG1-derived terminal sequences nucleate aragonite within peptide assemblies, albeit at low

dx.doi.org/10.1021/bi400808j | *Biochemistry* 2013, 52, 5696−5703

frequency.[45] It is likely that these isolated, shorter sequences now exhibit functional aberrations from their true roles within the parent protein. With that in mind, and in light of the present rPFMG1 study, we advise the reader to interpret our previous PFMG1 model peptide study[45] with caution and within the context of the current study.

We believe that protein oligomerization is critical to the PFMG1-mediated mineral amplification process (Figures 4 and 5). We discovered that the optimal formation of rPFMG1 assemblies occurs near the pI of the protein (pH 8.0, Figure 4) and in the presence of Ca^{2+} (Figure 5; Figures S6 and S7). This finding strongly suggests that protein electrostatics (i.e., side chain charge) is one of the driving forces for oligomerization. In addition, the detection of intrinsically disordered and aggregation-prone "interactive" sequences (Figures 1 and 6) makes a strong case for the participation of these sequences in oligomerization as well. Given that PFMG1 contains intrinsically disordered regions, it is not surprising that rPFMG1 oligomers adopt an amorphous morphology and are heterogeneous in dimension (Figures 4 and 5). We believe this is an important finding, for similar traits have been noted in other disordered biomineralization protein assemblies[4,9,11,12,23−25,38] and in disordered polymers that form mineral-stabilizing polymer-induced liquid phases (PILP).[46,47] Comparative mineralization studies of PILP polymers and biomineralization proteins will undoubtedly reveal if these disordered systems are mechanistically similar.

In addition to oligomerization, it is likely that the C-terminal EF-hand-like sequence (residues 61−110 Figure 1B) plays an important role in rPFMG1 nucleation enhancement. Our CD and bioinformatics studies indicate that this sequence does not share the same features and properties of the canonical EF-hand proteins. Rather, this sequence is qualitatively similar to the pseudo-EF-hand sequences found in SCaMCs (Figure 1).[19,21,22] However, this affiliation with SCaMCs is tempered by the occurrence of disordered and aggregation-prone sequences within the pseudo-EF-hand sequence of PFMG1 (Figure 1A). As a result of these alterations, we believe that the PFMG1 pseudo-EF-hand sequence region has been "tuned" to specifically function within the pearl mineralization scheme. For example, we speculate that the PFMG1 pseudo-EF-hand "imitator" sequence may be responsible for the Ca^{2+}-enhanced assembly of PFMG1 protein molecules (Figures 4 and 5; Figures S5 and S6). Alternatively, since PFMG1 protein oligomers would contain numerous pseudo-EF-hand domains concentrated within a limited molecular volume (Figures 4 and 5), these domains could play a role in the regulation of mineralization conditions (e.g., pH buffering, Ca^{2+} availability) in the vicinity of these protein oligomers. This, in turn, could significantly impact prenucleation cluster formation kinetics[41−43] and crystal quantities in solution (Figure 2). Obviously, other functions may be assignable to this domain, and additional studies will be required to establish the participation of the pseudo-EF-hand sequence within the oyster pearl mineralization process.

■ ASSOCIATED CONTENT

Supporting Information

MALDI-TOF spectra of purified rPFMG1 (Figure S1), SEM images of mineral deposits captured by Si wafers in mineralization assays (Figure S2), SEM and X-ray surface analyses of control and rPFMG1-treated crystals (Figures S3 and S4), DLS mass % plots for rPFMG1 as a function of pH and Ca^{2+}:protein mole ratios (Figures S5 and S6), and DLS analysis of rPFMG1 oligomerization (Figure S7). This material is available free of charge via the Internet at http://pubs.acs.org.

■ AUTHOR INFORMATION

Corresponding Author

*Tel (212) 998-9605; Fax (212) 995-4087; e-mail jse1@nyu.edu (J.S.E.).

Funding

This research was supported by the U.S. Department of Energy, Office of Basic Energy Sciences, Division of Materials Sciences and Engineering under Award DE-FG02-03ER46099.

Notes

The authors declare no competing financial interest.

■ ACKNOWLEDGMENTS

We thank Dr. Moise Ndao for performing the MALDI-TOF mass spectrometry analysis of rPFMG1. This report represents contribution number 67 from the Laboratory for Chemical Physics, New York University.

■ ABBREVIATIONS

PFMG1, PNC, DLS, SCaMC1, solute carrier mitochondrial carrier protein-1; S100, calcium binding protein that is 100% soluble in ammonium sulfate at neutral pH; CABP, calcium binding protein; FUTRAse, α-1,3-fucosyltransferase XI; PIBP, 1-phosphatidylinositol 4,5-bisphosphate phosphodiesterase Δ3A.

■ REFERENCES

(1) Shen, X., Belcher, A. M., Hansma, P. K., Stucky, G. D., and Morse, D. E. (1997) Molecular cloning and characterization of Lustrin A, a matrix protein from shell and pearl nacre of Haliotis rufescens. *J. Biol. Chem. 272*, 32472−32481.

(2) Samata, T., Hayashi, N., Kono, M., Hasegawa, K., Horita, C., and Akera, S. (1999) A new matrix protein family related to the nacreous layer formation of Pinctada fucata. *FEBS Lett. 462*, 225−232.

(3) Ma, Z., Huang, J., Sun, J., Wang, G., Li, C., Xi, L., and Zhang, R. (2007) A novel extrapallial fluid protein controls the morphology of nacre lamellae in the pearl oyster, Pinctada fucata. *J. Biol. Chem. 282*, 23253−23260.

(4) Suzuki, M., Saruwatari, K., Kogure, T., Yamamoto, Y., Nishimura, T., Kato, T., and Nagasawa, H. (2009) An acidic matrix protein, Pif, is a key macromolecule for nacre formation. *Science 325*, 1388−1390.

(5) Michenfelder, M., Fu, G., Lawrence, C., Weaver, J. C., Wustman, B. A., Taranto, L., and Evans, J. S. (2003) Characterization of two molluscan crystal-modulating biomineralization proteins and identification of putative mineral binding domains. *Biopolymers 70*, 522−533 errata 73, 522..

(6) Fu, G., Qiu, S. R., Orme, C. A., Morse, D. E., and DeYoreo, J. J. (2007) Acceleration of calcite kinetics by nacre proteins. *Adv. Mater. 17*, 2678−2683.

(7) Falini, G., Albeck, S., Weiner, S., and Addadi, L. (1996) Control of aragonite or calcite polymorphism by mollusk shell macromolecules. *Science 271*, 67−69.

(8) Ndao, M., Keene, E., Amos, F. A., Rewari, G., Ponce, C. B., Estroff, L., and Evans, J. S. (2010) Intrinsically disordered mollusk shell prismatic protein that modulates calcium carbonate crystal growth. *Biomacromolecules 11*, 2539−2544.

(9) Delak, K., Harcup, C., Lakshminarayanan, R., Zhi, S., Fan, Y., Moradian-Oldak, J., and Evans, J. S. (2009) The tooth enamel protein, porcine amelogenin, is an intrinsically disordered protein with an extended molecular configuration in the monomeric form. *Biochemistry 48*, 2272−2281.

(10) Mann, K., Siedler, F., Treccani, L., Heinemann, F., and Fritz, M. (2007) Perlinhibin, a cysteine, histidine, and arginine-rich miniprotein from abalone (*Haliotis laevigata*) nacre, inhibits in vitro calcium carbonate crystallization. *Biophys. J. 93*, 1246−1252.
(11) Amos, F. F., and Evans, J. S. (2009) AP7, a partially disordered pseudo C-RING protein, is capable of forming stabilized aragonite in vitro. *Biochemistry 48*, 1332−1339.
(12) Amos, F. F., Ndao, M., Ponce, C. B., and Evans, J. S. (2011) A C-RING-like domain participates in protein self-assembly and mineral nucleation. *Biochemistry 50*, 8880−8887.
(13) Uversky, V. N. (2002) Natively unfolded proteins: A point where biology waits for physics. *Protein Sci. 11*, 739−756.
(14) Tompa, P. (2002) Intrinsically unstructured proteins. *Trends Biochem. Sci. 27*, 527−533.
(15) Meng, J., Romero, P., Yang, J. Y., Chen, J. W., Vacic, V., Obradovic, Z., and Uversky, V. N. (2008) The unfoldomics decade: An update on intrinsically disordered proteins. *BMC Genomics 9*, 1−26.
(16) Chou, J. J., Li, S., Klee, C. B., and Bax, A. (2001) Solution structure of Ca(2+) calmodulin reveals flexible hand-like properties of its domains. *Nat. Struct. Biol. 8*, 990−997.
(17) Takeda, S., Yamashita, A., Maeda, K., and Maeda, Y. (2003) Structure of the core domain of human cardiac troponin in the Ca(2+)-saturated form. *Nature 424*, 35−41.
(18) Kojetin, D. J., Venters, R. A., Kordys, D. R., Thompson, R. J., Kumar, R., and Cavanagh, J. (2006) Structure, binding interface and hydrophobic transitions of Ca^{2+}-loaded calbindin-D(28k). *Nat. Struct. Mol. Biol. 13*, 641−647.
(19) Del Arco, A., and Satrustegui, J. (1998) Molecular cloning of Aralar, a new member of the mitochondrial carrier superfamily that binds calcium and is present in human muscle and brain. *J. Biol. Chem. 273*, 23327−23334.
(20) Nelson, M. R., Thulin, E., Fagan, P. A., Forsen, S., and Chazin, W. J. (2002) The EF-hand domina: a globally cooperative structural unit. *Protein Sci. 11*, 198−205.
(21) Traba, J., Del Arco, A., Duchen, M. R., Szabadkai, G., and Satrustegui, J. (2012) SCaMC-1 promotes cancer cell survival by desensitizing mitochondrial permeability transition via ATP/ADP-mediated matrix Ca(2+) buffering. *Cell Death Differ. 19*, 650−660.
(22) Del Arco, A., and Satrustegui, J. (2004) Identification of a novel human subfamily of mitochondrial carriers with calcium binding domains. *J. Biol. Chem. 279*, 24701−24713.
(23) Keene, E. C., Evans, J. S., and Estroff, L. A. (2010) Silk fibroin hydrogels coupled with the n16N-beta-chitin complex: An in vitro organic matrix for controlling calcium carbonate mineralization. *Cryst. Growth Des. 10*, 5169−5175.
(24) Amos, F. F., Ponce, C. B., and Evans, J. S. (2011) Formation of framework nacre polypeptide supramolecular assemblies that nucleate polymorphs. *Biomacromolecules 12*, 1883−1889.
(25) Ponce, C. B., and Evans, J. S. (2011) Polymorph crystal selection by n16, an intrinsically disordered nacre framework protein. *Cryst. Growth Des. 11*, 4690−4696.
(26) Schärtl, W. (2007) *Light Scattering from Polymer Solutions and Nanoparticle Dispersions* 1st ed., Springer-Verlag, Heidelberg, Germany.
(27) Nečas, D., and Klapetek, P. (2012) Gwyddion: an open-source software for SPM data analysis. *Cent. Eur. J. Phys. 10*, 181−188.
(28) Sreerama, N., and Woody, R. W. (2000) Estimation of protein secondary structure from circular dichroism spectra: Comparison of CONTIN, SELCON, and CDSSTR methods with an expanded reference set. *Anal. Biochem. 287*, 252−260.
(29) Lobley, A., Whitmore, L., and Wallace, B. A. (2002) DICHROWEB: An interactive website for the analysis of protein secondary structure from circular dichroism spectra. *Bioinformatics 18*, 211−212.
(30) Sreerama, N., and Woody, R. W. (2004) On the analysis of membrane protein circular dichroism spectra. *Protein Sci. 13*, 100−112.
(31) Zdobnov, E. M., and Apweiler, R. (2001) InterProScan an integration platform for the signature recognition methods in InterPro. *Bioinformatics 17*, 847−848.
(32) Arnold, K., Bordoli, L., Kopp, J., and Schwede, T. (2006) The SWISS-MODEL Workspace: A web-based environment for protein structure homology modeling. *Bioinformatics 22*, 195−201.
(33) Kiefer, F., Arnold, K., Künzli, M., Bordoli, L., and Schwede, T. (2009) The SWISS-MODEL Repository and associated resources. *Nucleic Acids Res. 37*, D387−D392.
(34) Dosztányi, Z., Csizmók, V., Tompa, P., and Simon, I. (2005) IUPred: web server for the prediction of intrinsically unstructured regions of proteins based on estimated energy content. *Bioinformatics 21*, 3433−3434.
(35) Ward, J. J., Sodhi, J. S., McGuffin, L. J., Buxton, B. F., and Jones, D. T. (2004) Prediction and functional analysis of native disorder in proteins from the three kingdoms of life. *J. Mol. Biol. 337*, 635−645.
(36) Linding, R., Russell, R. B., Neduva, V., and Gibson, T. J. (2004) A comparative study of the relationship between protein structure and beta-aggregation in globular and intrinsically disordered proteins (TANGO). *J. Mol. Biol. 342*, 345−353.
(37) Conchillo-Sole, O., de Groot, N. S., Aviles, F. X., Vendrell, J., Daura, X., and Ventura, S. (2007) AGGRESCAN: a server for the prediction and evaluation of "hot spots" of aggregation in polypeptides. *BMC Bioinformatics 8*, 65−82.
(38) Evans, J. S. (2012) Identification of intrinsically disordered and aggregation - promoting sequences within the aragonite-associated nacre proteome. *Bioinformatics 28*, 3182−3185.
(39) Ndao, M., Dutta, K., Bromley, K., Sun, Z., Lakshminarayanan, R., Rewari, G., Moradian-Oldak, J., and Evans, J. S. (2011) Probing the self-association, intermolecular contacts, and folding propensity of amelogenin. *Protein Sci. 20*, 724−734.
(40) Southgate, P., and Lucas, J. (2008) in *The Pearl Oyster: A Beginner's Guide to Programming Images, Animation, and Interaction* pp 77−102, Elsevier BV, Oxford, UK.
(41) Gebauer, D., Volkel, A., and Coelfen, H. (2008) Stable prenucleation of calcium carbonate clusters. *Science 322*, 1819−1822.
(42) Gebauer, D., and Coelfen, H. (2011) Prenucleation clusters and non-classical nucleation. *Nano Today 6*, 564−584.
(43) Demichelis, R., Raiteri, P., Gale, J. D., Quigley, D., and Gebauer, D. (2011) Stable prenucleation mineral clusters are liquid-like polymers. *Nat. Commun. 2*, 1−8.
(44) Gower, L. B. (2008) Biomimetic model systems for investigating the amorphous precursor pathway and its role in biomineralization. *Chem. Rev. 108*, 4551−4627.
(45) Amos, F. F., Destine, E., Ponce, C. B., and Evans, J. S. (2010) The N- and C-terminal regions of the pearl-associated EF Hand protein, PFMG1, promote the formation of the aragonite polymorph in vitro. *Cryst. Growth Des. 10*, 4211−4216.
(46) Wolf, E., Leiterer, J., Pipich, V., Barrea, R., Emmerling, F., and Tremel, W. (2011) Strong stabilization of amorphous calcium carbonate emulsion by ovalbumin Gaining insight into the mechanism of 'polymer-induced liquid precursor' processes. *J. Am. Chem. Soc. 133*, 12642−12649.
(47) Freeman, C. L., Harding, J. H., Quigley, D., and Rodger, P. M. (2010) Structural control of crystal nuclei by an eggshell protein. *Angew. Chem., Int. Ed. 49*, 5135−5137.